Title

Atmospheric mass-loss due to giant impacts: the importance of the thermal component for hydrogen–helium envelopes

Journal

Monthly Notices of the Royal Astronomical Society, 485(3)

ISSN

0035-8711

Authors

Biersteker, John B
Schlichting, Hilke E

Publication Date

2019-05-21

DOI

10.1093/mnras/stz738

Peer reviewed

Monthly Notices
of the
ROYAL ASTRONOMICAL SOCIETY

MNRAS **485,** 4454–4463 (2019)
Advance Access publication 2019 March 16

doi:10.1093/mnras/stz738

Atmospheric mass-loss due to giant impacts: the importance of the thermal component for hydrogen–helium envelopes

John B. Biersteker [1]★ and Hilke E. Schlichting [1,2]

[1] *Massachusetts Institute of Technology, 77 Massachusetts Avenue, Cambridge, MA 02139-4307, USA*
[2] *UCLA, 595 Charles E. Young Drive East, Los Angeles, CA 90095, USA*

Accepted 2019 March 7. Received 2019 March 7; in original form 2018 August 31

ABSTRACT

Systems of super-Earths and mini-Neptunes display striking variety in planetary bulk density and composition. Giant impacts are expected to play a role in the formation of many of these worlds. Previous works, focused on the mechanical shock caused by a giant impact, showed that these impacts can eject large fractions of the planetary envelope, offering a partial explanation for the observed compositional diversity. Here, we examine the thermal consequences of giant impacts, and show that the atmospheric loss caused by these effects can significantly exceed that caused by mechanical shocks for hydrogen–helium (H/He) envelopes. During a giant impact, part of the impact energy is converted into thermal energy, heating the rocky core and envelope. We find that the ensuing thermal expansion of the envelope can lead to a period of sustained, rapid mass-loss through a Parker wind, partly or completely eroding the H/He envelope. The degree of atmospheric loss depends on the planet's orbital distance from its host star and its initial thermal state, and hence age. Close-in planets and younger planets are more susceptible to impact-triggered atmospheric loss. For planets where the heat capacity of the core is much greater than the envelope's heat capacity (envelope mass fractions $\lesssim$4 per cent), the impactor mass required for significant atmospheric removal is $M_{\rm imp}/M_{\rm p} \sim \mu/\mu_{\rm c} \sim 0.1$, approximately the ratio of the heat capacities of the envelope and core. Conversely, when the envelope dominates the planet's heat capacity, complete loss occurs when the impactor mass is comparable to the envelope mass.

Key words: planets and satellites: atmospheres – planets and satellites: formation.

1 INTRODUCTION

A major discovery of the Kepler mission is the high abundance of planets intermediate in size between the Earth and Neptune with orbital periods less than 100 d (e.g. Borucki et al. 2011; Fressin et al. 2013; Petigura, Howard & Marcy 2013; Morton et al. 2016). These super-Earths and mini-Neptunes have no obvious Solar system analogue. Models of exoplanet structure and measurements of the bulk densities of these planets suggest that many possess hydrogen–helium (H/He) envelopes comprising several per cent of the planet's total mass (e.g. Adams, Seager & Elkins-Tanton 2008; Lopez & Fortney 2014; Weiss & Marcy 2014; Rogers 2015).

The accretion and evolution of super-Earth H/He envelopes have been studied extensively and can be broadly described by a three step process. First, planetary cores accrete their H/He envelopes from the protoplanetary nebula (e.g. Lee & Chiang 2015; Ginzburg, Schlichting & Sari 2016); second, the loss of pressure support from the surrounding nebula can lead the initially thermally inflated envelope to shed its outer layers, causing significant mass-loss (Ginzburg et al. 2016; Owen & Wu 2016); and third, photoevaporation by high-energy stellar radiation and the luminosity of the cooling core can erode the atmospheres of close-in planets (e.g. Lopez, Fortney & Miller 2012; Lopez & Fortney 2013; Owen & Wu 2013; Jin et al. 2014; Ginzburg, Schlichting & Sari 2018).

Although these processes successfully explain the observed valley in the distribution of small planet radii between 1.5–2 $R_\oplus$ (Fulton et al. 2017; Owen & Wu 2017; Fulton & Petigura 2018; Ginzburg et al. 2018; Gupta & Schlichting 2018), the exoplanet population appears to display more compositional diversity than predicted by these processes alone, suggesting additional mechanisms are at work. This is particularly the case for planets on orbits outside of ∼45 d, where photoevaporation and core cooling are less effective, and in multiplanet systems that host planets with dramatically different mean densities (see Fig. 1 and Inamdar & Schlichting 2016).

Evidence of additional processes can also be seen in the distribution of super-Earth envelope mass fractions in core mass versus equilibrium temperature phase space. Theoretical work on gas accretion (e.g. Lee & Chiang 2015; Ginzburg et al. 2016) predicts that the envelope mass fraction of a super-Earth should be determined

★ E-mail: jo22395@mit.edu

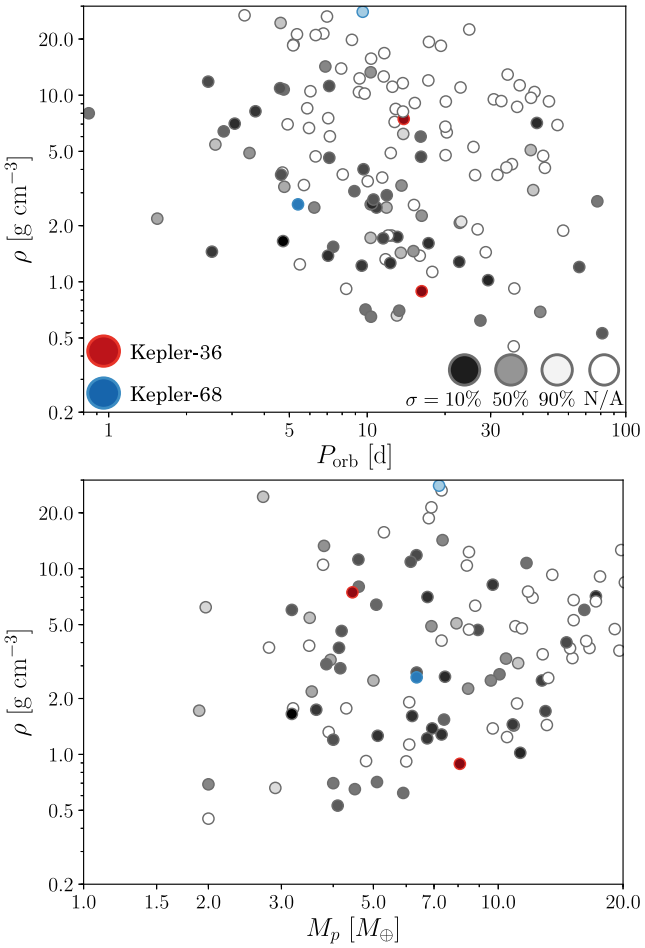

Figure 1. Bulk densities (ρ) of observed Kepler planets in multiplanet systems with radii $<4\,R_\oplus$ as a function of orbital period (P_{orb}) in the top panel, and total planet mass (M_p) in the bottom panel, after Inamdar & Schlichting (2016). Red and blue circles highlight Kepler-36 and Kepler-68, respectively, two examples of multiplanet systems with significant density contrast between planets. The transparency indicates the fractional uncertainty in the density, with darker points corresponding to greater certainty. In cases where the planet mass and radius are not provided in the same analysis, the uncertainty on the density is left undefined (N/A) and only an empty circle is plotted. Values are taken from the Composite Kepler planets table at the NASA Exoplanet Archive (June 2018).

by its equilibrium temperature and core mass, so that planets with the same envelope mass fraction should fall on distinct contours in a plot of planet mass versus equilibrium temperature, assuming no subsequent erosion of the atmosphere. However, this is not borne out by current observations. Instead, in the region of phase space where atmospheric mass-loss due to photoevaporation and core cooling is predicted to be unimportant, the exoplanet population exhibits no clear organization by envelope mass fraction (see fig. 6 and the 'global properties of super-Earth systems' section in Schlichting 2018). There are three possible reasons for this. First, there is significant uncertainty in the measured planet masses, possibly obscuring trends predicted by theoretical accretion models. Second, the accreted envelope fractions are expected to be a function of disc lifetime which varies somewhat from system to system. Finally, atmospheric loss that occurs after the gas disc disperses could erase any trends predicted from accretion. The observed exoplanet population is consistent with atmospheric erosion as planets are consistently found to have lower envelope fractions than predicted by atmospheric accretion models and envelope mass fractions do not appear to be correlated by planet mass and equilibrium temperature (Schlichting 2018).

One candidate process for altering planetary bulk densities and eroding planetary atmospheres is giant impacts. Giant impacts are believed to be the last major assembly stage in the formation of the terrestrial planets in our Solar system (e.g. Chambers 2001), and may also play a role in the formation of super-Earths (Hansen & Murray 2013; Inamdar & Schlichting 2015). Impacts, particularly those which occur after the dissipation of the gas disc, may significantly reduce the H/He envelopes of planets, or strip the cores entirely (Inamdar & Schlichting 2015; Liu et al. 2015; Schlichting, Sari & Yalinewich 2015; Inamdar & Schlichting 2016).

These late giant impacts may be a common occurrence during the formation of super-Earth systems because these planets form in the presence of the gas disc. The disc's dynamical interaction with the planets is expected to result in migration and efficient eccentricity damping, producing densely packed planetary systems. Once the gas disc dissipates and its damping effect is removed, these systems may not remain dynamically stable as the planets' eccentricities increase through secular excitation, possibly resulting in orbit crossing and giant impacts before regaining long-term orbital stability (Cossou et al. 2014; Izidoro et al. 2017; Denham et al. 2019). Because of the stochastic nature of giant impacts and the small number of impacts expected per system, atmospheric loss through late impacts may offer an especially attractive explanation for the compositional diversity observed among planets in the same system. In this paper, we return to the role of giant impacts in driving volatile loss from super-Earths and mini-Neptunes.

During a giant impact, the impactor is sharply decelerated and its kinetic energy is converted into heat which is deposited at the impact site, creating an event akin to a point-like explosion. This causes a strong shock that propagates through the planet and causes global ground motion, launching a shock into the planet's envelope. A series of previous studies of giant impacts have focused on the ejection of the atmosphere by this hydrodynamic shock (Genda & Abe 2003; Schlichting et al. 2015; Inamdar & Schlichting 2016). In addition, Liu et al. (2015) investigated volatile loss in two specific giant impact scenarios using 3D numerical simulation. They find that giant impacts can lead to significant loss of volatiles and point out that the atmospheric loss in their simulation is likely further enhanced by Parker winds and photoevaporation of the thermally inflated post-impact envelope.

In the case of H/He envelopes, the heating of the core during an impact can lead to significant mass-loss. Heat from the core is transferred to the envelope, either directly unbinding it, or leading to significant thermal expansion and gradual mass-loss via Parker winds. In this paper, we focus specifically on the thermal aspect of giant impacts, examining the energy of the impact, the thermal inflation of the H/He envelope after the impact, and the subsequent atmospheric loss. We demonstrate that the thermal component of atmospheric loss can dominate the loss caused by shocks for H/He atmospheres and that it may partly explain the observed compositional diversity in super-Earth systems. This paper is structured as follows: we begin with a model for the structure and evolution of a super-Earth envelope and core in Section 2, calculate the atmospheric mass-loss in a range of impact scenarios in Section 3, and conclude with a discussion in Section 4.

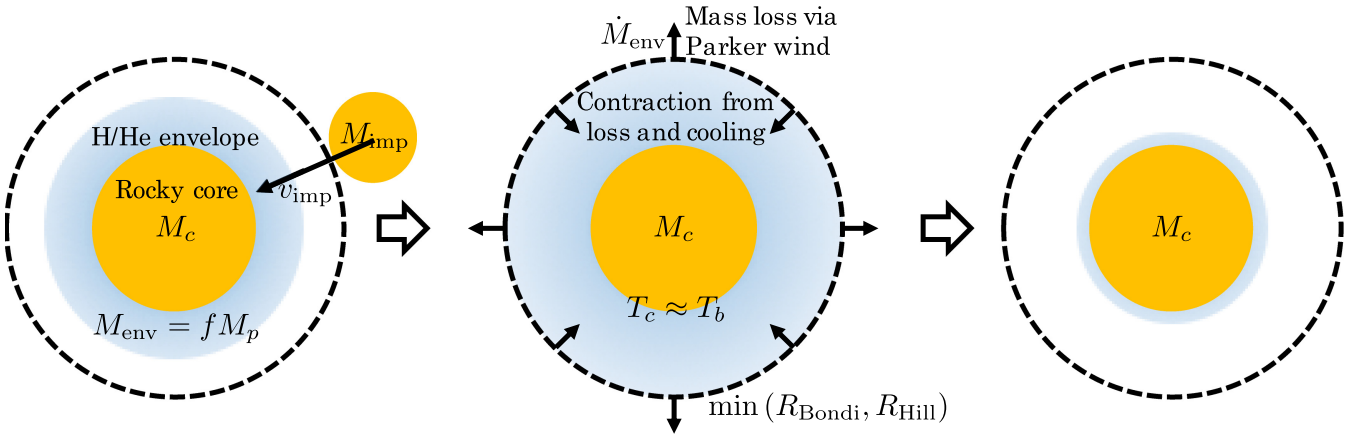

Figure 2. Schematic of atmospheric mass-loss following a giant impact. In the left-hand panel, an impactor with mass M_{imp} strikes a planet of mass M_p at impact velocity v_{imp}. The planet has a core mass of $M_c \approx M_p$ and envelope mass $M_{env} = fM_p$. In the middle panel, heat from the impact has inflated the envelope so that it loses mass through a Parker wind at its outer radius $R_{out} = \min(R_B, R_H)$. Mass-loss and cooling cause the envelope to contract, eventually halting appreciable atmospheric loss. At right, the planet is left to continue cooling with a significantly reduced envelope.

2 ENVELOPE STRUCTURE AND EVOLUTION

Giant impacts deposit significant energy into a planet's core and envelope, leaving the envelope in a thermally inflated state which can be highly susceptible to hydrodynamic escape (Fig. 2). The exact rate of mass-loss from the planetary envelope is determined by the atmospheric density at the outer edge of the envelope, where gas molecules are only tenuously gravitationally bound to the planet. This outer radius, R_{out}, is the lesser of the Bondi radius, $R_B = 2GM_p/c_s^2$, and the Hill radius, $R_H = a[M_p/(3M_{star})]^{1/3}$, where G is the gravitational constant, M_p is the planet mass, M_{star} is the stellar mass, a is the semimajor axis of the planet's orbit, and c_s is the sound speed of the gas. To determine the density at this radius, we first develop a simple model of the planet's envelope and core appropriate for conditions following a large impact. We then consider the evolution of this structure as the planet sheds mass, cools, and contracts to determine the total mass lost from the envelope.

2.1 Envelope structure model

We model the planet's envelope as an inner convective region with an adiabatic profile, and an outer radiative layer with an isothermal profile (see Rafikov 2006; Piso & Youdin 2014; Inamdar & Schlichting 2015; Ginzburg et al. 2016). In all the cases we consider here, the mass of the planet is dominated by the mass of the rocky core, so that $M_p \sim M_c$. Neglecting, therefore, the self-gravity of the envelope, the density, pressure, and temperature in the convective portion of the envelope are given by

$$\frac{\rho}{\rho_b} = \left[\frac{\gamma-1}{\gamma}\Lambda\left(\frac{R_c}{r}-1\right)+1\right]^{\frac{1}{\gamma-1}}, \quad (1)$$

$$\frac{P}{P_b} = \left[\frac{\gamma-1}{\gamma}\Lambda\left(\frac{R_c}{r}-1\right)+1\right]^{\frac{\gamma}{\gamma-1}}, \quad (2)$$

$$\frac{T}{T_b} = \frac{\gamma-1}{\gamma}\Lambda\left(\frac{R_c}{r}-1\right)+1, \quad (3)$$

where R_c is the core radius, r is the distance from the centre of the core, and γ is the adiabatic index of the envelope. We define Λ as approximately the ratio of the gravitational potential and kinetic energies of a gas particle at the base of the envelope, $\Lambda \equiv GM_c\mu/(R_c k_B T_b)$, where μ is the mean molecular weight of the envelope and k_B is the Boltzmann constant. The density, pressure, and temperature at the base of the envelope are ρ_b, P_b, and T_b, respectively.

At large enough radii, the atmospheric density decreases to the point that the envelope becomes radiative. In this region, the envelope is nearly isothermal with a temperature which is approximately the equilibrium temperature:

$$T_{eq} = \left(\frac{1-A_B}{4}\right)^{1/4}\sqrt{\frac{R_{star}}{a}}T_{star}, \quad (4)$$

where A_B is the Bond albedo, R_{star} is the stellar radius, and T_{star} is the star's effective temperature. Assuming the envelope outside this radiative–convective boundary (RCB) to be completely isothermal, the density profile of the envelope becomes exponential,

$$\rho = \rho_{rcb}\exp\left[\frac{R_{rcb}}{h}\left(\frac{R_{rcb}}{r}-1\right)\right], \quad (5)$$

with a scale height $h = k_B T_{eq} R_{rcb}^2/(GM_p\mu)$, where $r = R_{rcb}$ is the radius of the RCB and $\rho_{rcb} = \rho(R_{rcb})$. The pressure is then, using the ideal gas law, $P = \rho k_B T_{eq}/\mu$.

The mass in the convective region of the envelope is given by integrating equation (1):

$$M_{env} = 4\pi R_c^3 \rho_b \int_1^{x_{rcb}}\left[\nabla_{ad}\Lambda\left(\frac{1}{x}-1\right)+1\right]^{\frac{1}{\gamma-1}}x^2 dx, \quad (6)$$

where $x = r/R_c$, $x_{rcb} = R_{rcb}/R_c$, and $\nabla_{ad} \equiv (\gamma-1)/\gamma$. The energy of the envelope is determined from the gravitational and thermal energies, $E_{env} = E_g + E_{th}$, where the gravitational energy for a non-self-gravitating envelope is

$$E_g = -4\pi G M_c \rho_b R_c^2 \int_1^{x_{rcb}}\left[\nabla_{ad}\Lambda\left(\frac{1}{x}-1\right)+1\right]^{\frac{1}{\gamma-1}}x dx. \quad (7)$$

And the thermal energy is

$$E_{th} = 4\pi\rho_b R_c^3 \frac{k_B T_b}{\mu(\gamma-1)}\int_1^{x_{rcb}}\left[\nabla_{ad}\Lambda\left(\frac{1}{x}-1\right)+1\right]^{\frac{\gamma}{\gamma-1}}x^2 dx. \quad (8)$$

In cases considered in this paper, when T_b significantly exceeds T_{eq}, most of the envelope's mass is in the inner convective region. Ignoring the mass in the isothermal layer, the atmospheric structure is then entirely determined by the envelope mass (equation 6) and the envelope energy.

2.1.1 *Core model*

The planets we are considering are young (10–100 Myr) and have significant H/He envelopes. This allows them to retain significant heat from their formation so that the basal temperature of the envelope is $\gtrsim$2000 K, higher than the melting point of silicates. We therefore assume the core is undifferentiated, fully molten with no solid insulating crust, and that heat is efficiently transferred between the core and the base of the envelope so that the base temperature and core temperature are the same ($T_b \approx T_c$).

Adiabatic profiles of terrestrial planet interiors show changes in temperature of a factor of only a few over changes in depth of thousands of kilometers (Katsura et al. 2010), so we approximate the core as isothermal with an energy

$$E_c \sim c_{V,c} M_c T_c, \tag{9}$$

where $c_{V,c} \sim 5\text{–}10 \times 10^6$ erg g^{-1} K^{-1} is the specific heat capacity of the core (Guillot et al. 1995; Alfè, Price & Gillan 2001; Lopez et al. 2012). The specific heat capacity can be roughly approximated by $k_B/[\mu_c(\gamma_c - 1)]$ where μ_c and γ_c are the core's mean molecular weight and adiabatic index, respectively. In our numerical calculations, we adopt a value of $c_{V,c} = 7.5 \times 10^6$ erg g^{-1} K^{-1}. Finally, we adopt $R_c/R_\oplus \simeq (M_c/M_\oplus)^{1/4}$ as the core mass–radius relationship (e.g. Valencia, O'Connell & Sasselov 2006).

2.2 Envelope evolution

After an impact the envelope is inflated, enabling enhanced mass-loss. As the envelope cools and contracts, the density at the outer radius (R_{out}) drops, quenching the mass-loss. The thermal evolution of the envelope is driven by both radiation and the loss of energy through mass-loss (Owen & Wu 2016; Ginzburg et al. 2016, 2018). The mass-loss rate is approximately

$$\dot{M}_{env} \approx -4\pi R_{out}^2 \rho_{out} c_s, \tag{10}$$

where $c_s = \sqrt{\gamma k_B T/\mu}$ is the sound speed.

As can be seen from equation (1), the value of γ determines the shape of the density profile and therefore the distribution of mass in the envelope. We generally assume in this paper that $\gamma > 4/3$, which is valid for both monatmoic ($\gamma = 5/3$) and diatomic gases ($\gamma = 7/5$), and discuss the effect of choosing $\gamma < 4/3$ instead in Section 3.3. For $\gamma > 4/3$, equation (6) shows that the envelope mass is concentrated near the RCB. Raising a gas parcel from R_{rcb} to infinity requires a corresponding change in the envelope's energy,

$$\dot{E}_{env,m} \approx \frac{G M_c \dot{M}_{env}}{R_{rcb}}. \tag{11}$$

The planet also cools radiatively, with an approximate luminosity given by combining the equations of flux conservation and hydrodynamic equilibrium at the RCB:

$$\dot{E}_{env,L} = -L_{rcb} = -\nabla_{ad} \frac{64\pi\sigma T_{rcb}^3 G M_c \mu}{3\kappa_R \rho_{rcb} k_B}, \tag{12}$$

where σ is the Stefan–Boltzmann constant and κ_R is the Rosseland mean opacity of the envelope at the RCB. We adopt a value of $\kappa_R = 0.1$ cm^2 g^{-1} which is an appropriate approximation for the temperatures and conditions we expect at the RCB (Freedman, Marley & Lodders 2008).

The radiative flux from the RCB provides an upper limit on the mass-loss rate. When mass is lost from the envelope's outer edge (R_{out}) it is replaced by mass rising from the RCB. Energy must be supplied during this process in order to maintain the isothermal profile of the outer atmosphere. This energy is provided by a combination of the cooling luminosity of the planet (L_{rcb}) and stellar irradiation. We assume that the limit on the energy available to power this process is given by L_{rcb}, yielding a maximum mass-loss rate of

$$\dot{M}_{env,max} \approx -\frac{L_{rcb} R_{rcb}}{G M_c}. \tag{13}$$

This mass-loss rate should be regarded as an absolute upper limit since it assumes that any radiative losses are negligible and all of the cooling luminosity goes into driving the mass-loss (i.e. into mechanical work).

Combining the equations describing the envelope and core energies (equations 7, 8, and 9) yields the total energy $E = E_g + E_{th} + E_c$, which evolves by $\dot{E} = \dot{E}_{env,m} + \dot{E}_{env,L}$. The core mass is fixed and the envelope mass diminishes according to equation (10), unless this mass-loss rate exceeds the maximum rate, in which case the mass-loss is given by equation (13). As described in Section 2.1, the envelope structure is entirely determined by its mass and the energy of the system, so these equations are sufficient to describe the combined thermal and mass-loss evolution of the planet (Fig. 3).

3 MASS-LOSS FROM GIANT IMPACTS

Giant impacts during late planetary accretion can significantly alter the atmosphere of a nascent super-Earth. A large impact generates a shockwave which propagates through the planet, causing global ground motion which can immediately eject a fraction of the envelope (e.g. Schlichting et al. 2015). Additionally, the impactor delivers significant energy to the planet, heating the core, which in turn heats the envelope. The thermally inflated envelope can then be vulnerable to hydrodynamic escape and lose mass rapidly. Focusing on the thermal component of the mass-loss, we derive analytical estimates for both the time-scale of atmospheric loss and the impactor mass required to remove the atmosphere entirely. We then verify these estimates and explore a range of parameters using the numerical model described in Section 2.

3.1 Analytical estimates

3.1.1 *Complete atmospheric loss*

If an impactor delivers enough energy, a planet's gaseous envelope can be entirely removed. The energy required depends on the relative shares of the envelope and core in the energy budget of the planet. We estimate the critical envelope to core-mass fraction, f_*, for which the thermal energy stored in the core is comparable to the total energy of the envelope by equating the core's thermal energy (equation 9) to the total energy of the envelope. This yields

$$f_* \simeq \frac{(\gamma - 1)\mu c_{V,c}}{(\gamma + 1)k_B} \sim \frac{\mu}{\mu_c}, \tag{14}$$

where we used the approximation that $c_{V,c} \sim k_B/[\mu_c(\gamma_c - 1)]$ in the last expression. For $\mu = 2.3$ u, $\gamma = 7/5$, and $c_{V,c} = 7.5 \times 10^6$ erg K^{-1} g^{-1}, the resulting atmospheric mass fraction is $f_* \sim 0.04$.

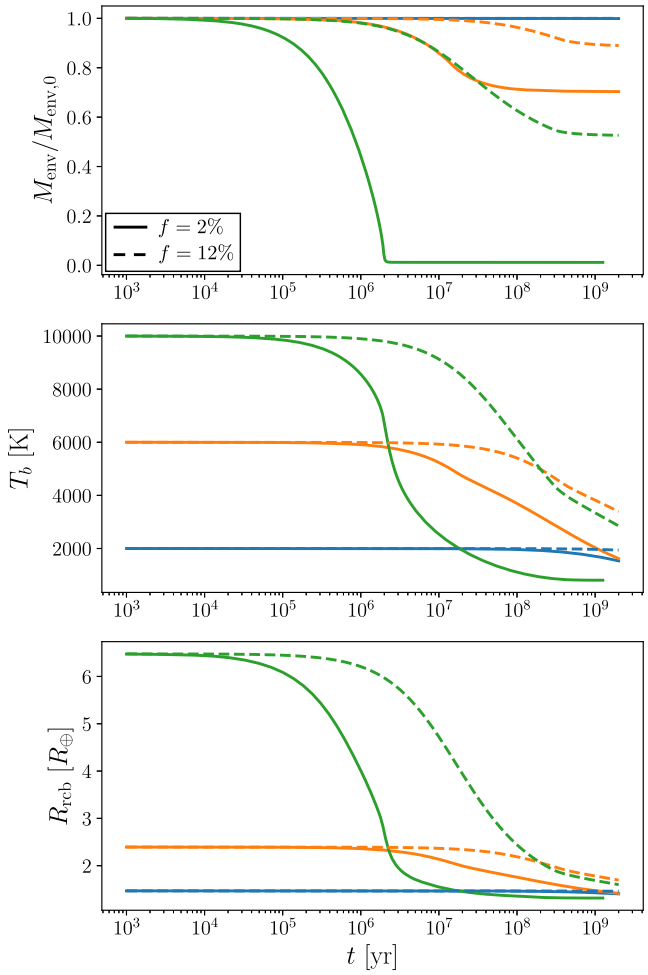

Figure 3. Examples of the evolution of the mass, base temperature, and RCB location of an H/He envelope for a planet with $M_{\rm c} = 3\,{\rm M}_\oplus$, $R_{\rm c} = 1.32\,{\rm R}_\oplus$, $a = 0.1$ au, $f = 2$ or 12 per cent, and a range of initial base temperatures, $T_{\rm b,0}$. The green, orange, and blue lines correspond, respectively, to initial base temperatures of 2000, 6000, and 10 000 K. The solid and dashed lines correspond to envelope mass fractions of $f = 2$ and 12 per cent.

In the limit where the core energy dominates ($f \ll f_*$), the envelope will be entirely lost in an impact when the temperature at the base of the envelope is so high that gas molecules do not remain gravitationally bound. Equivalently, the atmosphere is lost when the Bondi radius equals the core radius. Using the previously adopted core mass–radius relationship, $R_{\rm c}/{\rm R}_\oplus = (M_{\rm c}/{\rm M}_\oplus)^{1/4}$, this yields a required core temperature for complete loss of

$$T_{\rm c,crit} \simeq \frac{2\,G M_{\rm c}\mu}{\gamma k_{\rm B} R_{\rm c}} \simeq 25\,000\,{\rm K} \times \left(\frac{M_{\rm c}}{{\rm M}_\oplus}\right)^{3/4} \left(\frac{\mu}{2.3\,{\rm u}}\right) \left(\frac{7/5}{\gamma}\right). \quad (15)$$

The energy delivered by the impactor is $E_{\rm imp} = \eta M_{\rm imp} v_{\rm imp}^2/2$, where $\eta \in [0, 1]$ is the fraction of the total impact energy available for heating the core and envelope. Assuming an impact velocity $v_{\rm imp} \sim v_{\rm esc}$, the impact energy available for heating the core and envelope is then

$$E_{\rm imp} \simeq \eta M_{\rm imp} \frac{G M_{\rm p}}{R_{\rm c}}. \quad (16)$$

The corresponding impactor mass resulting in complete atmospheric loss for planets with $f \ll f_*$ is

$$M_{\rm imp} \simeq \frac{2\mu c_{V,{\rm c}}}{\eta\gamma k_{\rm B}} M_{\rm c} \sim \frac{1}{\eta}\frac{\mu}{\mu_{\rm c}} M_{\rm c}, \quad (17)$$

where we neglected any initial temperature of the core and, in the second expression, used the approximation that $c_{V,{\rm c}} \sim k_{\rm B}/[\mu_{\rm c}(\gamma_{\rm c} - 1)]$. The above equation implies that for planets whose heat capacity is dominated by the core, the impactor mass required for atmospheric loss is approximately given by the ratio of the mean molecular weights of the envelope and the core. This makes H/He envelopes particularly susceptible to loss. For an impact efficiency $\eta \sim 1$, equation (17) predicts total atmospheric loss for $M_{\rm imp} \sim 0.3 M_{\rm c}$ for $\mu = 2.3$ u, $\gamma = 7/5$, and $c_{V,{\rm c}} = 7.5 \times 10^6$ erg K^{-1} g^{-1}. We note here that equation (17) somewhat overestimates the impactor mass needed for complete atmospheric loss for very close-in planets. This is because equation (17) assumes that the envelope must be able to escape to infinity, while in reality it only has to be lifted out of the planet's potential well past the Bondi or the Hill radius.

When the initial, pre-impact, temperature of the core, T_0, is comparable to the temperature for complete loss, $T_{\rm c,crit}$, given in equation (15), then the impactor only needs to deliver enough energy to raise the core temperature by $\Delta T = T_{\rm c,crit} - T_0$. The corresponding impactor mass is then given by multiplying the right hand side of equation (17) by $\Delta T/T_{\rm c,crit}$. In the case of recently formed super-Earths which still retain significant heat from formation, ΔT may be small, so that complete atmospheric loss may occur for impactor masses significantly smaller than given by equation (17).

So far we discussed the limit in which $f \ll f_*$, we now turn to examining the case when the heat capacity of the core can be neglected, to first order, compared to that of the envelope ($f \gg f_*$). In this case, complete loss of the envelope occurs when the impact energy is comparable in magnitude to the energy of the envelope, i.e. when $E_{\rm imp} + E_{\rm env} = 0$. Approximating the envelope energy before the impact as $-GM_{\rm env}M_{\rm c}/R_{\rm c}$ and setting this equal to the impact energy given in equation (16), we find that complete loss occurs for an impactor mass of

$$M_{\rm imp} \simeq \frac{1}{\eta} M_{\rm env} \simeq \frac{f}{\eta} M_{\rm c}. \quad (18)$$

This implies that, for $\eta \sim 1$, the impactor mass must be comparable to the mass contained in the envelope.

3.1.2 *Partial atmospheric loss*

For impacts which do not immediately eject most of the planetary envelope, significant mass-loss is still possible as atmospheric loss from the inflated post-impact envelope can be driven by a Parker-type wind. Taking the mass-loss rate (equation 10) and the exponential density profile in the outer isothermal region (equation 5), the mass-loss time-scale, $\tau_{\rm loss}$ is

$$\tau_{\rm loss} \sim M_{\rm env}/\dot{M}_{\rm env} = \frac{M_{\rm env}}{4\pi R_{\rm out}^2 c_{\rm s} \rho_{\rm rcb}} \exp\left[\frac{R_{\rm rcb}}{h}\left(1 - \frac{R_{\rm rcb}}{R_{\rm out}}\right)\right]. \quad (19)$$

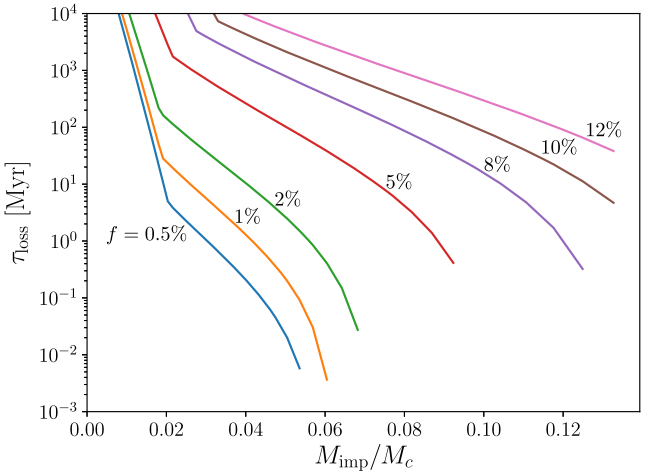

Figure 4. Estimated mass-loss time-scale ($\tau_{\rm loss}$) as a function of impactor mass ($M_{\rm imp}/M_{\rm c}$) for a range of H/He envelope mass fractions (f). The initial planet has $M_{\rm c} = 3\,{\rm M}_\oplus$, $R_{\rm c} = 1.32\,{\rm R}_\oplus$, $T_{\rm b,0} = 2000$ K, $a = 0.1$ au. The abrupt change in slope in each curve is caused by mass-loss rate reaching the maximum loss rate given by equation (13).

In the case that $R_{\rm out}$ is given by the Bondi radius ($R_{\rm B}$), the expression becomes

$$\tau_{\rm loss} \sim \frac{M_{\rm env}}{4\pi R_{\rm B}^2 c_{\rm s} \rho_{\rm rcb}} \exp\left[\frac{\gamma}{2}\left(\frac{R_{\rm B}}{R_{\rm rcb}} - 1\right)\right],$$

and when $R_{\rm out} = R_{\rm H}$, the time-scale is given by

$$\tau_{\rm loss} \sim \frac{M_{\rm env}}{4\pi R_{\rm H}^2 c_{\rm s} \rho_{\rm rcb}} \exp\left[\frac{\gamma}{2}\left(\frac{R_{\rm B}}{R_{\rm rcb}} - \frac{R_{\rm B}}{R_{\rm H}}\right)\right].$$

The exponential dependence on $R_{\rm rcb}/R_{\rm out}$ indicates that the mass-loss time-scale is highly sensitive to changes in the location of the RCB relative to either the Bondi or the Hill radius. Therefore, modest changes in the impactor mass, which determines the new atmospheric base temperature, and hence $R_{\rm rcb}$, and the semimajor axis, which determines $R_{\rm out}$, will strongly affect the mass-loss rate (see Fig. 4). Eventually the mass-loss rate reaches the maximum rate at which the outer envelope's isothermal profile can be maintained (equation 13). In this case, the mass-loss time-scale given in equation (19) must be replaced by $\tau_{\rm loss} \sim M_{\rm env}/\dot{M}_{\rm env,max} \sim G M_{\rm c} M_{\rm env}/(R_{\rm c} L_{\rm rcb})$, resulting in less dramatic changes in the loss time-scale with impactor mass (see Fig. 4).

Significant atmospheric loss will occur as long as the mass-loss time-scale is short compared to the cooling time-scale of the envelope. Equation (19) guarantees rapid envelope loss when $R_{\rm out} \sim R_{\rm rcb}$, which yields a temperature requirement of

$$T_{\rm c} \simeq T_{\rm eq}\left[1 + \left(\frac{R_{\rm B}}{R_{\rm c}} - \frac{R_{\rm B}}{R_{\rm out}}\right)\frac{(\gamma-1)}{2}\right], \quad (20)$$

and a corresponding impactor mass of

$$M_{\rm imp} \simeq \frac{1}{\eta}\nabla_{\rm ad}\frac{c_{V,{\rm c}}\mu}{k_{\rm B}}\left(\frac{R_{\rm c}}{R_{\rm rcb,0}} - \frac{R_{\rm c}}{R_{\rm out}}\right)M_{\rm c}$$
$$\simeq \frac{1}{\eta}\frac{\mu}{\mu_{\rm c}}\left(\frac{R_{\rm c}}{R_{\rm rcb,0}} - \frac{R_{\rm c}}{R_{\rm out}}\right)M_{\rm c}, \quad (21)$$

where the zero subscript indicates the value prior to impact. For planets with $M_{\rm c} = 3\,{\rm M}_\oplus$, $a = 0.1$ au, and $T_{\rm b,0} = 2000$ K (as in Fig. 4) the impactor must raise the core temperature to $\sim 10^4$ K for rapid loss, corresponding to an impactor mass of $\sim 0.15\,{\rm M}_\oplus$, or $\sim 0.05 M_{\rm c}$.

Significant atmospheric loss is therefore expected to occur for much lower impactor masses than required for complete loss (compare equations 17 and 21). Over time the envelope cools as it loses energy through both mass-loss and radiation. Whether the mass-loss can proceed until the envelope is completely lost depends on the relative magnitudes of the cooling and mass-loss time-scales. For planets with core-dominated energy budgets, the reservoir of energy provided by the core can maintain the envelope in an inflated state, so that rapid mass-loss can continue. Since in this case the total energy $E \sim E_{\rm c}$, the base temperature of the envelope will remain roughly $T_{\rm c} \sim E_{\rm c}/(c_{V,{\rm c}} M_{\rm c})$ even as the envelope is lost. Therefore in this regime near total atmospheric loss is expected in giant impacts involving impactor masses given by equation (21).

3.2 Results

To determine the mass-loss in a range of impact scenarios and verify our analytical results, we perform numerical integrations of the equations governing the evolution of the envelope and core (Section 2.2) for a variety of planetary parameters and impactors. At each step in an integration, the envelope structure is recomputed from the current envelope mass and the envelope and core energies. The derivative dE/dt is determined by equations (11) and (12), and d$M_{\rm env}$/dt given by equations (10) or (13) as appropriate. We use the ODEINT function provided by SCIPY for these calculations.

We define the total mass-loss fraction, X, as the fraction of the envelope's mass lost after 2 Gyr of integration. By 2 Gyr after the impact, contraction of the envelope will have substantially reduced the mass-loss rate, so that any additional loss is negligible (Fig. 3). Unless otherwise stated, we assume a sunlike star, a core with $M_{\rm c} = 3\,{\rm M}_\oplus$, $R_{\rm c}/{\rm R}_\oplus = (M_{\rm c}/{\rm M}_\oplus)^{1/4} = 1.32\,{\rm R}_\oplus$, and a pre-impact core temperature of $T_{\rm c,0} = 2000$ K. We assume the H/He envelope has $\mu = 2.3$ u and $\gamma = 7/5$, with an atmospheric base temperature that is determined by the core temperature, $T_{\rm b,0} = T_{\rm c,0}$. We consider a range of semimajor axes and envelope mass fractions, and impactor masses ranging from approximately 0.01–0.5 ${\rm M}_\oplus$. We assume that, initially, all the impact energy goes into heating the core, corresponding to an efficiency of $\eta = 1.0$. Additionally, we assume an impact velocity of $v_{\rm imp} = v_{\rm esc}$. The first assumption is an overestimate, while the second is likely an underestimate. We discuss the implications of these parameter choices in Section 3.3.

For the reference case, we take $a = 0.1$ au and investigate envelope mass fractions ranging from $f = 0.5$–12 per cent. The final mass-loss for these scenarios is shown in Fig. 5. We find that atmospheric loss is remarkably efficient. Specifically, depending on f, impactor masses of $\sim$0.1–0.4 ${\rm M}_\oplus$, or $\sim$0.03–0.15 $M_{\rm c}$, are sufficient to completely remove the envelope. For comparison, we include in Fig. 5 the approximate loss caused by hydrodynamic shocks from Schlichting et al. (2015) assuming the same impact velocity ($v_{\rm imp} = v_{\rm esc}$).[1] For this size impactor, the hydrodynamic escape caused by thermal expansion is significantly more important than found in previous studies of the shock-induced losses (Schlichting et al. 2015; Inamdar & Schlichting 2016, 2015).

The higher efficiency of thermal atmospheric loss compared to shock-induced loss can be intuitively understood as follows. For the shock launched by the impactor to completely remove the envelope, the impact has to deliver enough energy and momentum

[1]The expression here broadly reproduces the results from a more thorough treatment (Inamdar & Schlichting 2015, 2016) and is sufficiently accurate for our purposes.

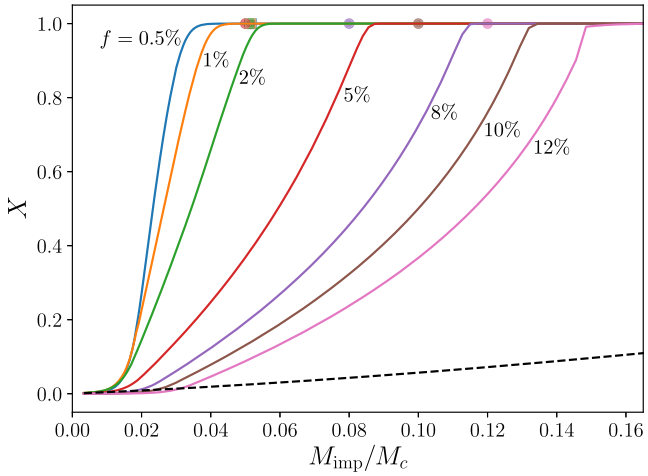

Figure 5. Mass fraction of H/He envelope lost (X) as a function of impactor mass ($M_{\rm imp}/M_{\rm c}$) for a planet with $M_{\rm c} = 3\,{\rm M}_\oplus$, $R_{\rm c} = 1.32\,{\rm R}_\oplus$, $T_{\rm b,0} = 2000$ K, $a = 0.1$ au, and a range of envelope mass fractions (f). Square and circular marks at $X = 1$ show the analytically derived impactor mass required for total mass-loss from equations (21) and (18) for core- and envelope-dominated energy budgets, respectively. The black dashed line indicates the atmospheric envelope loss from shocks during the impact (equation 33, Schlichting et al. 2015) assuming $v_{\rm imp} \sim v_{\rm esc}$.

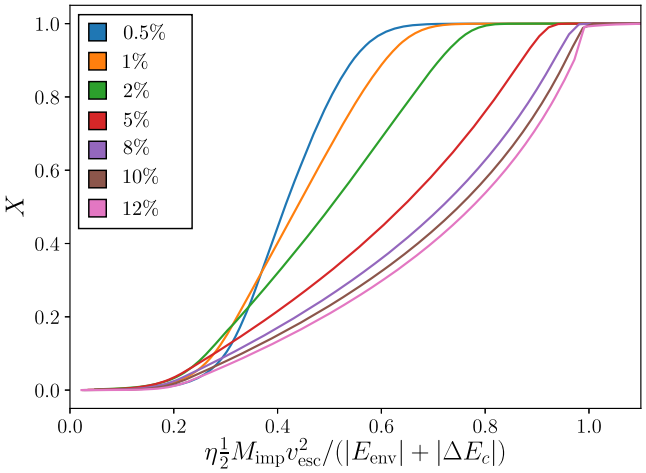

Figure 6. Mass fraction of H/He envelope lost (X) as a function of normalized impactor energy for a planet with $M_{\rm c} = 3\,{\rm M}_\oplus$, $R_{\rm c} = 1.32\,{\rm R}_\oplus$, $T_{\rm b,0} = 2000$ K, $a = 0.1$ au, and a range of envelope mass fractions (f). The impactor energy is normalized to the sum of the envelope energy ($E_{\rm env}$), calculated from equations (7) and (8), and the energy required to heat the core to the temperature in equation (20) ($\Delta E_{\rm c}$).

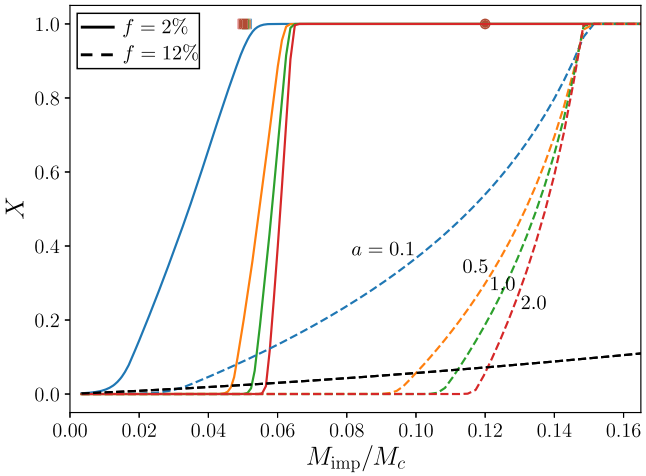

Figure 7. Mass fraction of H/He envelope lost (X) as a function of impactor mass ($M_{\rm imp}/M_{\rm c}$) for a planet with $M_{\rm c} = 3\,{\rm M}_\oplus$, $R_{\rm c} = 1.32\,{\rm R}_\oplus$, $T_{\rm b,0} = 2000$ K, $f = 2$ or 12 per cent, and a range of orbital radii (a). Square and circular marks at $X = 1$ show the analytically derived impactor mass required for total mass-loss from equations (21) and (18) for core- and envelope-dominated energy budgets, respectively. The black dashed line indicates the atmospheric envelope loss from shocks during the impact (equation 33, Schlichting et al. 2015) assuming $v_{\rm imp} \sim v_{\rm esc}$.

for the ground velocity resulting from the shock as it emerges at the antipode to be comparable to the escape velocity of the planet (for a rough estimate see equation 28 in Schlichting et al. 2015). For $v_{\rm imp} = v_{\rm esc}$, this requires impactor masses comparable to the target mass. In contrast, when considering atmospheric losses from the thermal heating of the envelope after the impact, the impact only needs to heat the core to temperatures that yield thermal velocities of the atmosphere sufficient for loss. For H/He atmospheres, this requires less energetic impacts than needed for shock induced volatile loss (see equations 17 and 18).

We find rough agreement between our analytical estimates for the required impactor mass (equations 18 and 21) and our numerical results. In general, our approximate values underestimate the required impactor mass because they are derived for the limiting cases where the energy of the envelope or core can be ignored to first order. In reality, the impact energy goes into both the thermal expansion of the envelope and heating the core. Including both the finite core and envelope masses by normalizing the impact energy by the envelope energy and core energy deficit, $E_{\rm env} + \Delta E_{\rm c}$, we find that the normalized energy required for atmospheric loss is similar across all envelope mass fractions, as shown in Fig. 6. The envelope energy is calculated from equations (7) and (8) and $\Delta E_{\rm c}$ is the energy required to heat the core to the temperature in equation (20).

The analytical expressions overestimate the impactor mass for complete loss in one case: planets on close ($a \lesssim 0.1$ au) orbits with low-mass envelopes. Close-in planets have relatively small Bondi/Hill's radii and, because of their higher equilibrium temperatures, larger exponential scale heights ($h \propto t_{\rm eq}$). As a consequence, the effect of the exponential decrease in atmospheric density is less severe at the outer radius, and rapid mass-loss is possible with lower impactor masses.

As a planet's orbital separation increases, $R_{\rm out}$ ($R_{\rm H}$ or $R_{\rm B}$) also increases so that an impact can inflate the envelope without leading to significant mass-loss. As shown in Fig. 7, this increases the impactor mass required to initiate significant atmospheric loss substantially, but does not dramatically change the impactor mass required for complete loss. As a result, the impactor mass required to initiate loss becomes closer to the mass required for complete ejection, and the range of impactor masses producing intermediate results shrinks, so that most impacts produce binary outcomes – either complete loss or no loss (Figs 7 and 8).

While this binarity is more pronounced at greater orbital separations, even at $a = 0.1$ au the range of impactor masses producing partial envelope loss is relatively narrow. The difference between negligible and total atmospheric loss for a given planet is typically a factor of ~2–4 in impactor mass, depending on the envelope mass. Regardless of orbital distance, lower mass envelopes have

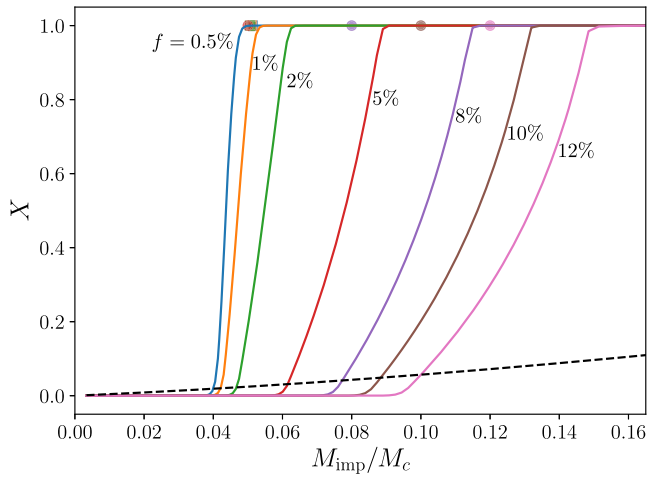

Figure 8. Mass fraction of H/He envelope lost (X) as a function of impactor mass ($M_{\rm imp}/M_{\rm c}$) for a planet with $M_{\rm c} = 3\,{\rm M}_\oplus$, $R_{\rm c} = 1.32\,{\rm R}_\oplus$, $T_{\rm b,0} = 2000$ K, $a = 0.5$ au, and a range of envelope mass fractions (f). Square and circular marks at $X = 1$ show the analytically derived impactor mass required for total mass-loss from equations (21) and (18) for core- and envelope-dominated energy budgets, respectively. The black dashed line indicates the atmospheric envelope loss from shocks during the impact (equation 33, Schlichting et al. 2015) assuming $v_{\rm imp} \sim v_{\rm esc}$.

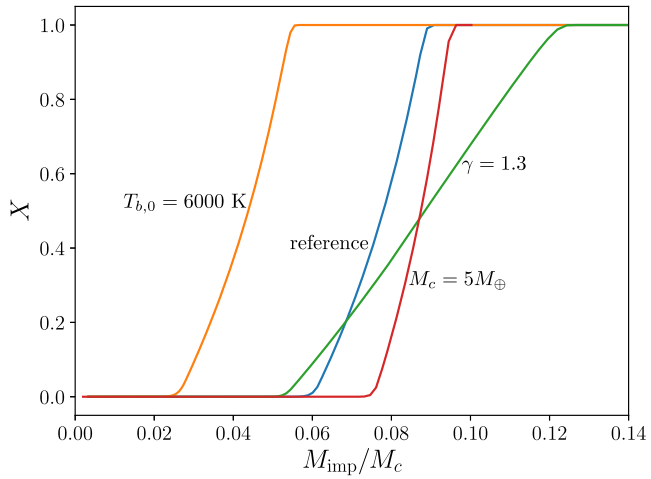

Figure 9. Mass fraction of H/He envelope lost (X) as a function of impactor mass ($M_{\rm imp}/M_{\rm c}$) under multiple scenarios. The reference scenario is in blue and corresponds to $M_{\rm c} = 3\,{\rm M}_\oplus$, $R_{\rm c} = 1.32\,{\rm R}_\oplus$, $a = 0.5$ au, $f = 5$ per cent, $T_{\rm b,0} = 2000$ K, and $\gamma = 7/5$. The orange line corresponds to $T_{\rm b,0} \rightarrow 6000$ K, the green curve to $\gamma \rightarrow 1.3$, and the red line to $M_{\rm c} \rightarrow 5\,{\rm M}_\oplus$, while all other parameters match the reference case.

a narrower range of intermediate outcomes and are more likely to entirely lose or retain their envelopes (Figs 5, 7, and 8).

3.3 Importance of parameter choices and model assumptions

In the results presented here, we have assumed certain properties for the impact scenario and impacted super-Earth. We test the effect of changing γ, $T_{\rm b,0}$, and $M_{\rm c}$ to determine the sensitivity of our results to our choice of parameters for the target super-Earth (Fig. 9). Dissociation of molecular hydrogen in the accreting and cooling envelopes of super-Earths and mini-Neptunes can result in values of $\gamma < 4/3$, typically ranging from 1.2 to 1.3 (Lee, Chiang & Ormel 2014; Lee & Chiang 2015; Inamdar & Schlichting 2016). We therefore performed a set of calculations with a value of $\gamma = 1.3$ instead of 7/5. This modifies the density profile of the envelope (see equation 1) so that the envelope mass is now concentrated near the core instead of the $R_{\rm rcb}$. Therefore, for this calculation, the expression for the cooling due to mass-loss (equation 11) is replaced by $GM_{\rm c}\dot{M}_{\rm env}/R_{\rm c}$. In addition, the change in the envelope's mass distribution in the $\gamma = 1.3$ case required us to implement a mass-loss treatment for the case when $R_{\rm rcb} > R_{\rm out}$. This condition generally does not occur for $\gamma > 4/3$ because those envelopes are lost before the impactors are large enough to produce this outcome. To approximate the mass lost in this overflow phase, we calculate the energy of a hypothetical impact (ΔE) that corresponds to $R_{\rm rcb} \simeq R_{\rm out}$ and for which the envelope is just bound (i.e. $E_{\rm env} \sim 0$). We then determine the difference between the actual impact energy and energy that yields $E_{\rm env} \sim 0$ and assume that this surplus energy produces mass-loss according to

$$M_{\rm env,lost} \approx \frac{\left(E_{\rm imp} - \Delta E\right) R_{\rm c}}{GM_{\rm c}}. \quad (22)$$

After this overflow phase, the remaining envelope has $R_{\rm rcb} \lesssim R_{\rm out}$ and its thermal evolution and further mass-loss are calculated according to the model described in Section 2. Because the envelope loses more energy per unit of mass lost for $\gamma = 1.3$ compared to $\gamma = 7/5$, larger impactor masses are required to remove the entire envelope. Setting $\gamma = 1.3$ also increases the envelope's heat capacity, causing it to receive a larger share of the impact energy. This allows the envelope to begin losing mass at lower impact energies than in the reference case. Both of these effects can be seen in Fig. 9.

Changes in the base temperature and core mass produce results consistent with expectations from equations (18) and (21). Increasing the base temperature of the envelope significantly reduces the impact energy (mass) required to inflate the envelope to the point of atmospheric loss. And, at a fixed f, increasing the core mass slightly increases the required impactor-to-core mass ratio ($M_{\rm imp}/M_{\rm c}$) for complete loss. This is because increasing the core mass expands the outer radius while shrinking the portion of the envelope which is convective, resulting in a greater exponential drop in the atmospheric density at the outer radius ($R_{\rm B}$ or $R_{\rm H}$) and higher impactor masses to achieve significan t atmospheric loss.

We also examine the sensitivity to changes in the impact scenario. In our default scenario, we have conservatively taken $v_{\rm imp} = v_{\rm esc}$. This is valid, however, only in the case of zero relative velocity between the planet and the impactor when they are widely separated. Accounting for this velocity at infinity yields $v_{\rm imp}^2 = v_{\rm esc}^2 + v_\infty^2$, where a realistic value for the initial relative velocity in the final stages of terrestrial planet formation is $v_\infty \approx v_{\rm esc}$ (Wetherill 1976; O'Brien, Morbidelli & Levison 2006). The result is a doubling of the impact energy expected from a particular event, corresponding to achieving the same atmospheric loss with half the impactor mass.

Conversely, the assumption that $\eta = 1$, i.e. all of the impact energy is available for heating the core and envelope, yields an upper bound on the thermal atmospheric mass-loss. In a real impact, the impact energy is divided into potential, kinetic, and internal energy according to the details of the collision. Only the internal energy is available for heating, and only a portion of that internal energy will be converted to heat, with some energy lost to other processes, such as phase transitions. Models of a range of Moon-forming impact scenarios suggest that after the shock and decompression

phase, 40–60 per cent of the impact energy is left in internal energy (Carter, Lock & Stewart 2018). Taking a heating efficiency of $\eta \sim 0.5$ as typical, then the thermal energy of the impact is roughly half what we have assumed above, and the impactor mass required to produce those effects must be doubled. Impacts which do not result in mergers deposit less energy in the target, resulting in even lower values of η. These events can be common in environments which are dynamically excited ($v_\infty \gtrsim v_{esc}$) (e.g. Asphaug 2010). But, two bodies which experience such a collision are likely to re-encounter one another, ultimately resulting in an accretionary impact where the bulk of the impact energy is deposited in the target.

The impact velocity and heating efficiency of the impact set the total energy available to power the thermal atmospheric loss, and therefore strongly affect the final outcome. The results presented here, which are equivalent to a choice of $v_\infty \sim v_{esc}$ and $\eta \sim 0.5$, are representative of typical outcomes up to a factor of a few. The range of typical outcomes, however, is large and a factor of ∼2–4 change in the thermal energy can make the difference between negligible and complete atmospheric loss (Fig. 6).

4 DISCUSSION AND CONCLUSIONS

We have shown that the thermal expansion of an H/He envelope after a giant impact can lead to a period of rapid mass-loss which can substantially erode the atmosphere. We find that, for impactors with a mass ∼10 per cent of the planet mass, this mechanism can reduce the envelope mass by ∼50–100 per cent. For planets where the thermal energy of the core is much greater than the envelope energy, the impactor mass required for significant atmospheric removal is $M_{imp}/M_c \sim \mu/\mu_c \sim 0.1$. This result is only weakly dependent on the atmospheric mass fraction. In contrast, when the envelope energy dominates the total energy budget, the impactor mass required to remove the envelope increases with the envelope mass fraction, $M_{imp} \propto M_{env}$. In all cases, however, we find that for H/He envelopes the thermal loss mechanism significantly exceeds the immediate atmospheric loss from impact-generated shocks, which only yields a loss fraction of ∼10 per cent for $\sim 0.1 M_p$ mass impactors (e.g. Inamdar & Schlichting 2016).

Our analysis does not include the effect of hydrogen outgassing from the interior of the planet, either directly from the magma ocean or through volcanism, which may act to buffer the atmospheric loss (Chachan & Stevenson 2018). We also neglect additional atmospheric mass-loss through XUV photoevaporation, which will be enhanced for these planets as a result of their inflated envelopes. The mass-loss reported here will therefore be an underestimate, though the effect of photoevaporation will be less important for planets with larger semimajor axes (Owen & Wu 2017).

The addition of the thermal component of impact-driven atmospheric loss may help to explain the observed diversity in planetary compositions, particularly for planets on orbits outside ∼45 d, where photoevaporation and core cooling are less effective, or in systems where neighbouring planets display large density contrasts. Systems of super-Earths are expected to undergo a phase of giant impacts after the dispersal of the gas disc, roughly 10–100 Myr after their initial formation (Cossou et al. 2014; Izidoro et al. 2017). Inamdar & Schlichting (2016) show that the atmospheric loss due to mechanical shocks caused by impacts between similarly sized bodies can change a planet's bulk density by a factor of 2–3. They suggest this process as an explanation for the observed diversity in planetary bulk density. We show that the thermal component of the impact should dominate the atmospheric loss of these planets, greatly enhancing the efficiency of atmospheric stripping from impacts. This is especially the case for these impacts because, at an age of 10–100 Myr, the planetary cores should still retain significant heat from their formation, reducing the impact energy needed to inflate the envelope. Our results suggest that a single large ($\sim 0.1 M_p$) impact is sufficient to remove an H/He atmosphere entirely. Assuming the envelope has a thickness comparable to the core radius, so that $R_p \sim 2R_c$ (e.g. Lopez & Fortney 2014; Ginzburg et al. 2016), complete atmospheric loss would result in a factor of ∼8 change in the bulk density.

Atmospheric mass-loss is sensitive to the details of the impact scenario (Section 3.3). Because these details are stochastic, and because the post-disc instability produces a small number of giant impacts per system (Izidoro et al. 2017), impact-driven mass-loss may therefore naturally explain the observed diversity of super-Earth densities.

ACKNOWLEDGEMENTS

We thank James Owen for valuable comments that helped to improve the manuscript. HES gratefully acknowledges support from the National Aeronautics and Space Administration under grant No. 17-XRP17_2-0055 issued through the Exoplanets Research Program. This research made use of the software packages NUMPY (Van Der Walt, Colbert & Varoquaux 2011), SCIPY G45, ASTROPY (Astropy Collaboration 2013), and MATPLOTLIB (Hunter 2007). Additionally, this research has made use of the NASA Exoplanet Archive, which is operated by the California Institute of Technology, under contract with the National Aeronautics and Space Administration under the Exoplanet Exploration Program.

REFERENCES

Adams E. R., Seager S., Elkins-Tanton L., 2008, ApJ, 673, 1160
Alfè D., Price G. D., Gillan M. J., 2001, Phys. Rev. B, 64, 045123
Asphaug E., 2010, Chemie der Erde – Geochem., 70, 199
Astropy Collaboration, 2013, A&A, 558, A33
Borucki W. J. et al., 2011, ApJ, 736, 19
Carter P. J., Lock S. J., Stewart S. T., 2018, LPI Contrib., 2083, 2731
Chachan Y., Stevenson D. J., 2018, ApJ, 854, 21
Chambers J. E., 2001, Icarus, 152, 205
Cossou C., Raymond S. N., Hersant F., Pierens A., 2014, A&A, 569, A56
Denham P., Naoz S., Hoang B.-M., Stephan A. P., Farr W. M., 2019, MNRAS, 482, 4146
Freedman R. S., Marley M. S., Lodders K., 2008, ApJS, 174, 504
Fressin F. et al., 2013, ApJ, 766, 81
Fulton B. J., Petigura E. A., 2018, AJ, 156, 264
Fulton B. J. et al., 2017, AJ, 154, 109
Genda H., Abe Y., 2003, Icarus, 164, 149
Ginzburg S., Schlichting H. E., Sari R., 2016, ApJ, 825, 29
Ginzburg S., Schlichting H. E., Sari R., 2018, MNRAS, 476, 759
Guillot T., Chabrier G., Gautier D., Morel P., 1995, ApJ, 450, 463
Gupta A., Schlichting H. E., 2018, preprint (arXiv:1811.03202)
Hansen B. M. S., Murray N., 2013, ApJ, 775, 53
Hunter J. D., 2007, Comput. Sci. Eng., 9, 90
Inamdar N. K., Schlichting H. E., 2015, MNRAS, 448, 1751
Inamdar N. K., Schlichting H. E., 2016, ApJ, 817, L13
Izidoro A., Ogihara M., Raymond S. N., Morbidelli A., Pierens A., Bitsch B., Cossou C., Hersant F., 2017, MNRAS, 470, 1750
Jin S., Mordasini C., Parmentier V., van Boekel R., Henning T., Ji J., 2014, ApJ, 795, 65
Jones E., Oliphant T., Peterson P., et al., 2001, SciPy: Open source scientific tools for Python, Available at:http://www.scipy.org/
Katsura T. et al., 2010, Phys. Earth Planet. Inter., 183, 212
Lee E. J., Chiang E., 2015, ApJ, 811, 41
Lee E. J., Chiang E., Ormel C. W., 2014, ApJ, 797, 95

Liu S.-F., Hori Y., Lin D. N. C., Asphaug E., 2015, ApJ, 812, 164
Lopez E. D., Fortney J. J., 2013, ApJ, 776, 2
Lopez E. D., Fortney J. J., 2014, ApJ, 792, 1
Lopez E. D., Fortney J. J., Miller N., 2012, ApJ, 761, 59
Morton T. D., Bryson S. T., Coughlin J. L., Rowe J. F., Ravichandran G., Petigura E. A., Haas M. R., Batalha N. M., 2016, ApJ, 822, 86
Owen J. E., Wu Y., 2013, ApJ, 775, 105
Owen J. E., Wu Y., 2016, ApJ, 817, 107
Owen J. E., Wu Y., 2017, ApJ, 847, 29
O'Brien D. P., Morbidelli A., Levison H. F., 2006, Icarus, 184, 39
Petigura E. A., Howard A. W., Marcy G. W., 2013, Proc. Natl. Acad. Sci., 110, 19273
Piso A.-M. A., Youdin A. N., 2014, ApJ, 786, 21
Rafikov R. R., 2006, ApJ, 648, 666
Rogers L. A., 2015, ApJ, 801, 41
Schlichting H., 2018, Formation of Super-Earths., Springer, Cham, 141
Schlichting H. E., Sari R., Yalinewich A., 2015, Icarus, 247, 81
Valencia D., O'Connell R. J., Sasselov D., 2006, Icarus, 181, 545
Van Der Walt S., Colbert S. C., Varoquaux G., 2011, Comput. Sci. Eng., 13, 22
Weiss L. M., Marcy G. W., 2014, ApJ, 783, L6
Wetherill G. W., 1976, in Merrill R. B., ed., LPI Contrib., 1573, 3245

This paper has been typeset from a TEX/LATEX file prepared by the author.